

STRUCTURE OF TiB_2 PRODUCED BY DYNAMIC ION MIXING*

J. P. RIVIERE, PH. GUESDON, J. DELAFOND and M. F. DENANOT

Laboratoire de Métallurgie Physique, Faculté des Sciences, 40 avenue du Recteur Pineau, 86022 Poitiers (France)

(Received May 31, 1988)

Summary

The new technique of dynamic ion mixing is based on the use of a high energy ion beam to homogenize at the atomic scale and to improve the adherence of a growing film on any substrate. TiB_2 films of stoichiometric composition are produced either by co-evaporation or by dynamic ion mixing using 100 keV Ar^+ ions. The characterization of the films is performed by transmission electron microscopy (TEM).

The results indicate that the ion mixing of the growing film has a crucial importance with regard to the resulting microstructural state. Amorphous TiB_2 films are produced by conventional co-evaporation although crystalline TiB_2 films of hexagonal structure are produced by dynamic ion mixing. The TiB_2 amorphous phase appears to be very stable since crystallization starts only at about 1170 K, and complete transformation into the hexagonal crystalline structure is obtained at 1280 K. Relatively thick TiB_2 coatings have been prepared with $e = 1 \mu\text{m}$ and studied by TEM on cross-sectional preparations. The microhardness of crystalline TiB_2 films is about 2800 kgf mm^{-2} and is in good agreement with the value reported for bulk TiB_2 .

1. Introduction

Ion implantation and ion beam mixing of pre-evaporated multilayers have proved to be very convenient and powerful methods for producing new metastable alloys. They offer the possibility of changing the mechanical or physical properties of a surface in a very controlled and reproducible way without the constraints of thermodynamic phase equilibrium. Along the path of the implanted ion, a highly disordered region is produced consisting of many displacements and replacements resulting in a severe atomic rearrangement.

*Paper presented at the Symposium on the Preparation and Properties of Metastable Alloys at the E-MRS Spring Meeting, Strasbourg, May 31 - June 2, 1988.

In coating technology, film adhesion to the substrate is an important requirement, and it is achieved in the above methods by means of the cascade mixing effect through the film-substrate interface. However, because of the limited ion range in matter, the coating thickness formed by conventional ion mixing does not generally exceed 100 nm. Such thin layers are insufficient for most practical applications although long-lasting improvements in wear resistance have been observed many times but are not well understood.

Several groups are developing a new approach to improving the coating adherence or increasing the coating thickness by combining a deposition technique with the ion bombardment. From the point of view of the ion beam energy used to assist or enhance the deposition, there are two classes of techniques. In the first and most important, low energy ion beams are used, typically in the range 1 - 10 keV [1 - 4]. The major disadvantage of these methods is that the energy is deposited in a very small volume near the surface, limiting the mixing effect and consequently the adhesion improvement. However, the growing demand for thicker coatings of precisely defined composition and structure has led to the development of new techniques using ion beams of higher energy in the range 40 - 200 keV [5, 6].

The use of ion implantation in thin film deposition guarantees a low background pressure in the vicinity of the substrate and allows a high degree of control in the energy deposited in the target.

The reproducibility of film production together with the good adhesion to the substrate are important factors for potential applications. With this process, it is thought that a new range of material compositions could be obtained. We have designed an ultrahigh-vacuum system with two electron gun evaporators operating in line with a 200 kV ion implanter.

In this paper, we present the preliminary results of an investigation on the structure and properties of TiB_2 films produced by dynamic ion mixing.

2. Experimental techniques

2.1. *Dynamic ion mixing apparatus*

The dynamic ion mixing apparatus used in this work is shown schematically in Fig. 1. It is composed of a cylindrical ultrahigh vacuum chamber equipped with two 8 kW electron beam evaporators. The base pressure before evaporation is 10^{-7} - 10^{-8} Pa and is obtained by sorption, cryogenic and ion pumping, and a titanium sublimator. In addition, the sample holder is surrounded by a cold wall held at 77 K to avoid sample contamination. The pressure is always lower than 10^{-6} Pa during evaporation experiments.

The rotating sample holder is positioned at an angle of 45° with respect to the ion beam and also to the vertical axis, allowing continuous evaporation and implantation. In order to maintain a high degree of control over the deposition rates from both sources, the two electron guns are automatically

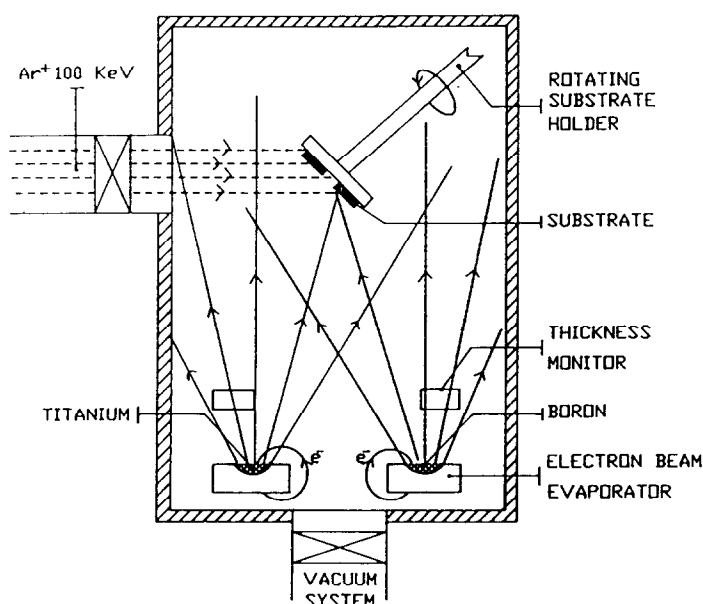


Fig. 1. Schematic representation of the dynamic ion beam mixing apparatus under ultra-high vacuum.

and independently controlled via two calibrated quartz crystal oscillators giving also a precise thickness measurement. Because ultrahigh vacuum systems are sophisticated, their utilization is tedious and time consuming, and for this reason the apparatus has been designed with an intermediary isolated chamber associated with a sample manipulator which allows successive introduction and extraction of samples without breaking the vacuum inside the evaporation chamber.

2.2. Experimental conditions

The distance between the evaporators and the substrate is 200 mm and the deposition temperature is about 300 K. In order to obtain the desired composition for the stoichiometric compound TiB_2 , we have chosen in a first experiment a titanium evaporation rate equal to 5 \AA s^{-1} and for boron 4.3 \AA s^{-1} . The ion beam mixing is performed with 100 keV Ar^+ ions. The characteristic parameters of the ion implantation, *i.e.* ion and damage ranges, and deposited energy, have been calculated with the TRIM computer code [7] and are given in Table 1. The total ion fluence for mixing is $0.8 \times 10^{15} \text{ ions cm}^{-2}$ for 100 nm thick films and $8 \times 10^{15} \text{ ions cm}^{-2}$ for 1 μm thick films. In the latter case, the deposition-implantation duration, is exactly 17 min 49 s and the ion:atom arrival rate ratio is 0.7×10^{-4} .

2.3. Substrates and characterization

The thinnest films of 100 nm are deposited on freshly cleaved NaCl crystals. They are ready for transmission electron microscopy (TEM) obser-

TABLE 1

Calculated implantation parameters in TiB_2 for a 45° angle of incidence

<i>Ion</i>	<i>E</i> (keV)	<i>E_D</i> (keV)	$\langle x_p \rangle$	$\langle \Delta x_p \rangle$ (nm)	$\langle x_D \rangle$ (nm)	$\langle \Delta x_D^2 \rangle^{1/2}$ (nm)	$\langle Y_D^2 \rangle^{1/2}$ (nm)	θ_D (ev atom ⁻¹)
⁴⁰ Ar	100	50	45.7	19.4	40.1	24.2	9.8	6.2×10^{-2}

E_D is the damage energy transferred by an ion of incident energy E , and $\langle x_p \rangle$ and $\langle \Delta x_p \rangle$ are the mean ion range and straggling. $\langle x_D \rangle$ is the mean damage range, and $\langle \Delta x_D^2 \rangle^{1/2}$ and $\langle Y_D^2 \rangle^{1/2}$ are the longitudinal and transversal damage straggling. θ_D is the elastic energy deposited per target atom in the displacement cascade.

vations after the NaCl substrate is dissolved in water. Thicker coatings (1 μm) were deposited by ion mixing on different substrates: tungsten carbide (WC), stainless steel and silicon. The shape of these specimens is rectangular (25 mm \times 17 mm) and they are 2 mm thick. Before the deposition, these substrates were given an initial dose of about 10^{14} ions cm^{-2} for surface cleaning.

Composition depth profiles obtained by secondary ion mass spectrometry (SIMS) indicate a flat and uniform titanium and boron concentration through the coating. TEM observations were also performed on cross-sectional preparations in the case of 1 μm thick films deposited on silicon or stainless steel. Some Vickers' microindentation tests were also carried out for the hardness determination of the coating.

3. Experimental results

3.1. Structure of unimplanted TiB_2 films

The diffraction pattern of a thin TiB_2 film produced without ion beam bombardment is presented in Fig. 2(a). Only diffuse rings are visible and it is possible to detect on the second ring a typical shoulder. These observations indicate that a completely amorphous structure of the TiB_2 film has been obtained. A transmission electron micrograph taken in bright field conditions is given in Fig. 2(b). We can notice a uniform contrast characteristic of an amorphous structure. The latter is a metastable phase and it is important to know the critical temperature above which crystallization occurs.

The thermal evolution of amorphous TiB_2 has been studied. The specimens were mounted on molybdenum grids and heated in the electron microscope at a rate of about 10 K min^{-1} . The TiB_2 amorphous phase is very stable since absolutely no transformation occurs up to 1170 K. Figure 3 illustrates the final state at the crystallization process. Crystallization starts at 1170 K and complete transformation to the crystalline hexagonal structure is observed at 1250 K. The lattice parameter c is found to be 3.18 Å and the reported value is 3.22 Å [8]. The lattice parameter a is estimated to be

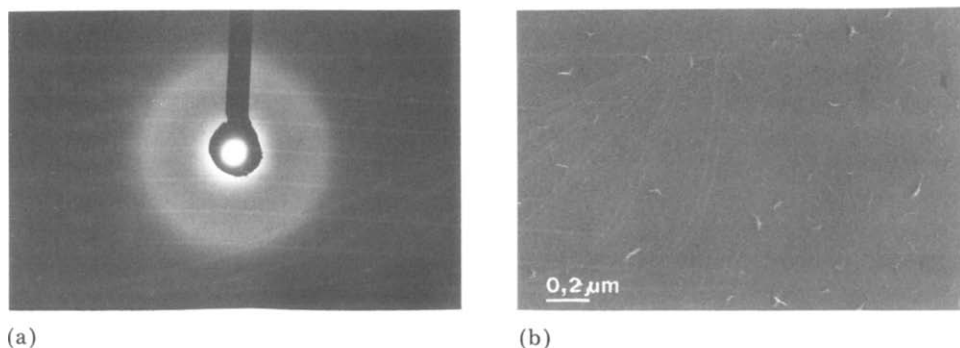


Fig. 2. (a) Electron diffraction pattern of an unimplanted TiB_2 film. The diffuse rings are characteristic of the amorphous state. (b) Transmission electron micrograph of amorphous TiB_2 .

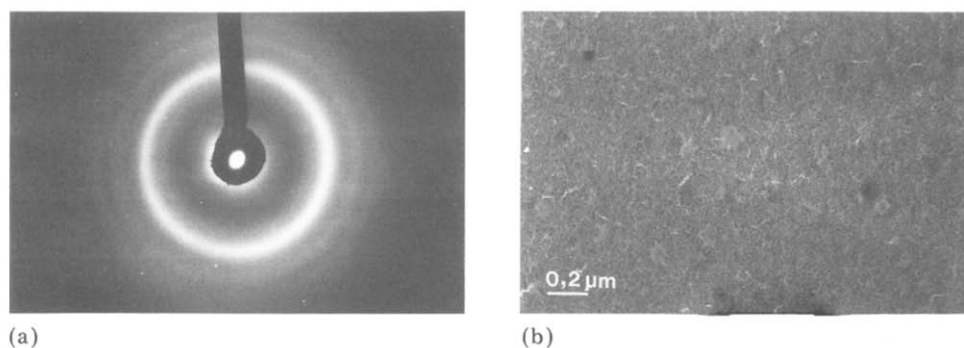


Fig. 3. (a) Electron diffraction pattern after crystallization of amorphous TiB_2 . The structure is hexagonal ($a = 3.02 \text{ \AA}$, $c = 3.18 \text{ \AA}$). (b) Transmission electron micrograph of crystalline TiB_2 . The amorphous-to-crystalline transformation occurs in the range 1170 - 1280 K.

about 3.02 \AA and the reported value is 3.02 [8]. These experimental values are in good agreement with the reported values within the experimental accuracy.

3.2. Structure of TiB_2 produced by dynamic ion mixing

Two series of TiB_2 specimens have been prepared and studied. In the first series, the films are 100 nm thick and studied by plan TEM; the second series consists of thicker films ($1 \text{ }\mu\text{m}$) deposited on either silicon or stainless steel substrates and cross-sectional preparations have been used in this case.

The microstructural state of the thinnest TiB_2 films prepared by dynamic ion mixing at a dose of $0.8 \times 10^{15} \text{ ions cm}^{-2}$ is shown in Fig. 4(a). The corresponding selected area diffraction pattern is given in Fig. 4(b). One can notice that it does not exhibit diffuse rings as in unimplanted films (Fig. 2(b)); on the contrary, sharp Debye-Scherrer concentric rings are present, indicating a crystalline structure with very small disoriented grains. The

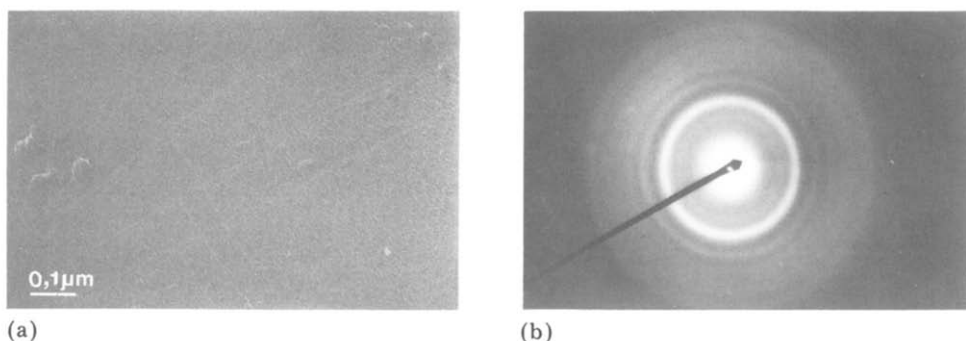


Fig. 4. (a) Transmission electron micrograph of crystalline TiB_2 produced by dynamic ion mixing. (b) Electron diffraction pattern of crystalline TiB_2 produced by dynamic ion mixing. The absence of $(000n)$ diffraction rings should be noted.

hexagonal TiB_2 phase could be identified. However, it should be noticed on the diffraction pattern of Fig. 4(b) that the reflections $(000n)$ are absent, suggesting that the film has a strong preferred orientation in the $[0001]$ direction. Such behaviour has already been observed several times for TiB_2 crystalline films prepared by other methods [9, 10]. The values determined ($a = 3.02 \text{ \AA}$ and $c = 3.18 \text{ \AA}$) are identical to those reported in Section 3.1. Transmission electron micrographs of cross-sections of a $1 \mu\text{m}$ TiB_2 coating prepared by dynamic ion mixing with a dose of $8 \times 10^{15} \text{ ions cm}^{-2}$ are presented in Fig. 5 in bright and dark field conditions. The selected area diffraction patterns show the surface to be crystalline TiB_2 . In this case, it was possible to identify all the reflections of the hexagonal structure without any ambiguity. Moreover, examination of the TiB_2 layer reveals the columnar structure and confirms the previous observation concerning the preferred orientation.

3.3. Mechanical properties of TiB_2 coatings

Vickers' microindentation tests have been carried out with low loads of 25 - 75 gf on TiB_2 coatings of $1 \mu\text{m}$ thickness deposited by dynamic ion mixing on WC. The determination of the intrinsic microhardness of such a thin layer is difficult. The measurements give the property of a composite material composed of the layer plus the substrate when the layer thickness is not about 10 times the indentation depth. Several models have been proposed [11, 12] to calculate the hardness of a composite specimen consisting of a thin layer on a substrate.

From the measurements of the effective hardness of both the composite and the substrate it is possible as proposed by Jönsson [12] to deduce the layer hardness value. We have summarized in Table 2 the results of such a determination. It is found that the characteristic microhardness of the crystalline TiB_2 coating is about 2800 kgf mm^{-2} and this value agrees well with other reported values for this compound [9, 10, 13]. Preliminary scratch tests using a loaded diamond stylus indicate that the TiB_2 coating

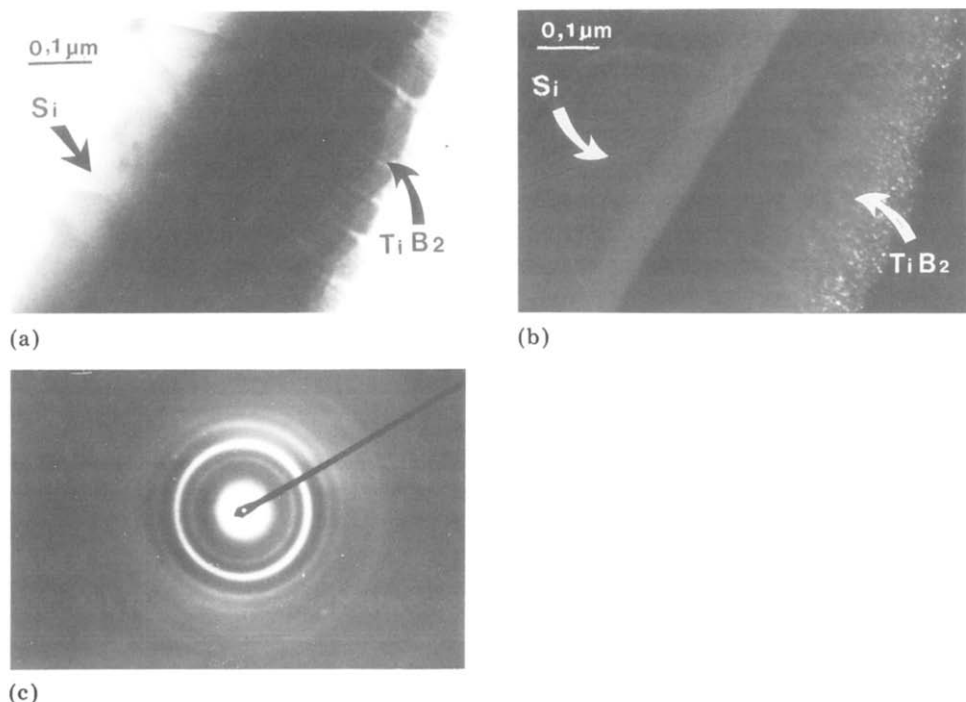


Fig. 5. (a) Transmission electron micrograph in bright field conditions of a cross-section of a 1 μm polycrystalline TiB_2 film deposited by dynamic ion mixing (Ar^+ ; 100 keV; dose, 8×10^{15} ions cm^{-2}). (b) Transmission electron micrograph in dark field conditions corresponding to (a). (c) Selected area diffraction pattern showing the surface film to be crystalline TiB_2 .

TABLE 2

Microhardness results

Load (gf)	Substrate hardness (kgf mm^{-2})	Coating plus substrate hardness (kgf mm^{-2})	TiB_2 coating hardness (kgf mm^{-2})
75	1006 ± 30	1166 ± 30	2730 ± 700
50	913 ± 40	1121 ± 40	2840 ± 730
25	715 ± 50	1021 ± 50	2815 ± 750

adhesion to the substrate is greatly improved by the dynamic ion mixing process. It seems reasonable to assume that it is the consequence of the ion mixing of the interface with the substrate in the first stage of the film deposition.

4. Discussion

The results presented here demonstrate that dynamic ion mixing is capable of depositing relatively thick, uniform and adherent crystalline TiB_2 coatings. These experiments provide also clear evidence of the role of the high energy ion beam bombardment during deposition of a growing film since TiB_2 is obtained in an amorphous form by codeposition alone and in a crystalline form by dynamic ion mixing. Although no detailed study has yet been carried out on the relative influence of the different implantation parameters such as dose, energy or temperature, the dynamic ion mixing method would be able to produce coatings of well-controlled composition and crystalline structure as demonstrated for stoichiometric TiB_2 .

It is difficult to give at present a comprehensive description of all the processes involved in this method. However, it is reasonable to assume that the basic processes of growth phenomena and ion beam mixing are combined. From the point of view of the film growth, experimental and theoretical studies indicate that the movement of adatoms over the surface is of major importance. Under the ion bombardment, the surface mobility of atoms could be modified by the defect production and atomic rearrangements that accompany the bombardment. Large numbers of defects (about 1088 defects per incident argon ion in TiB_2) are produced in the near-surface region and it is possible that even at room temperature their mobility stimulates or enhances the atomic transport, facilitating the surface diffusion since the surface acts as an efficient defect sink. In this way, the build-up of the crystalline surface would be promoted.

Even if defects are not effectively mobile, molecular dynamic simulations indicate that in the third stage of the dynamic cascade an important fraction of the initial energy is distributed in the form of kinetic energy of interstitials as well as in non-permanently displaced atoms [14]. For high energy deposition values in the cascade, thermal spike effects provide also another possible explanation of defect mobility in the near-surface region as previously suggested by Armour *et al.* [15].

The formation of crystalline TiB_2 by dynamic ion mixing could appear in apparent contradiction with the fact that ion implantation produces non-equilibrium structures. However, it is also known that crystallization can be induced by irradiation at temperatures much lower than those required for a purely thermal process as observed for instance in NiAl [16]. Radiation-induced crystallization can be understood on the basis of nucleation enhanced inside the displacement cascades and growth enhanced via the high defect concentrations which increase the diffusion rate. In the case of dynamic ion mixing it is possible to suggest that the high density of localized atomic displacements produced in the first cascades at the beginning of the film deposition would act as preferential nucleation sites for the crystalline TiB_2 phase.

The structural effects in thin films produced by ion bombardment during deposition have been discussed by Harper *et al.* [2] in terms of

universal parameters such as the ion:atom arrival rate ratio as a function of energy in the case of low ion energies. It has been demonstrated that this factor has an important role in reducing the internal stress in thin films. In the present study with 100 keV Ar⁺ ions the ion:atom arrival rate ratio is 0.7×10^{-4} and, according to the analysis of Harper *et al.* this value is in the good regime of operation for modifications to be expected during deposition.

5. Conclusion

The use of high energy ion beam to realize thick coatings by dynamic ion mixing is of fundamental and technological interest. It is expected that the high degree of control of the process could be applied to produce films of desired structure and compositions of hard ceramic materials. The basic phenomena of film growth under ion bombardment are not well understood and further investigations of the influence of the different parameters involved in the process are necessary.

Acknowledgments

The authors wish to thank C. Boisseaux for his technical assistance during dynamic ion mixing experiments, J. P. Desmaison for the scratch tests (Université Limoges), and M. Cahoreau and J. Caisso for SIMS depth profiles.

References

- 1 J. J. Cuomo and S. M. Rossmagel, *Nucl. Instrum. Methods B*, 19 - 20 (1987) 963.
- 2 J. M. E. Harper, J. J. Cuomo, R. J. Gambino and H. R. Kaufman, *Nucl. Instrum. Methods B*, 7 - 8 (1985) 886.
- 3 N. A. G. Ahmed, J. S. Colligon and A. E. Hill, *Thin Solid Films*, 117 (1984) 223.
- 4 G. Fisher, A. E. Hill and J. S. Colligon, *Vacuum*, 28 (1978) 277.
- 5 Y. Andoh, Y. Suzuki, K. Matsuda, M. Satou and F. Fujimoto, *Nucl. Instrum. Methods B*, 6 (1985) 111.
- 6 R. A. Kant, B. D. Sartwell, I. L. Singer and R. G. Vardiman, *Nucl. Instrum. Methods* 209 - 210 (1984) 915.
- 7 J. P. Biersack and L. G. Hagmark, *Nucl. Instrum. Methods*, 174 (1980) 257.
- 8 Joint Committee on Powder Diffraction Standards, *Powder Diffraction File*, sets 6 - 10, 1967, p. 310, card 8-121 (Joint Committee on Powder Diffraction Standards, Philadelphia, PA).
- 9 T. Shikawa, Y. Sakai, M. Fukutomi and M. Okada, *Thin Solid Films*, 156 (1988) 287.
- 10 R. F. Bunshah, R. Nimmagadda, W. Dunford, B. A. Movchan, A. V. Demchishin and N. A. Chunsanov, *Thin Solid Films*, 54 (1978) 85.
- 11 A. Wagendristel, H. Bandert, X. Cai and A. Kaminitschah, *Thin Solid Films*, 154 (1987) 199.
- 12 B. Jönsson and S. Hogmark, *Thin Solid Films*, 114 (1984) 257.
- 13 J. T. Prater, *Surf. Coat. Technol.*, 29 (1986) 247.

- 14 M. M. Guinan and J. H. Kinney, *J. Nucl. Mater.*, 103 - 104 (1981) 1319.
- 15 D. G. Armour, P. Bailey and G. Sharples, *Vacuum*, 36 (11 - 12) (1986) 769.
- 16 J. Delafond, C. Jaouen, J. P. Riviere and C. Fayoux, *Mater. Sci. Eng.*, 69 (1985) 117.